



# Synthesis of activated carbon from cherry tree waste and its application in removing cationic red 14 dye from aqueous environments

Roya Askari<sup>1,2</sup> · Faezeh Mohammadi<sup>1,2</sup> · Amir Moharrami<sup>1,2</sup> · Shirin Afshin<sup>1,2</sup> · Yousef Rashtbari<sup>1,2</sup> · Mehdi Vosoughi<sup>1,3</sup> · Abdollah Dargahi<sup>4,3</sup>

Received: 4 February 2023 / Accepted: 16 February 2023 / Published online: 6 March 2023  
© The Author(s) 2023

## Abstract

The environment is threatened by a diversity of pollutants, and synthetic dyes are considered a foremost environmental pollutant among them. The characteristics detected for the dye, e.g., toxicity and carcinogenicity, have brought severe problems for humans and aquatic organisms. The present study was done to clarify the potential of activated carbon made from cherry tree wood (CWAC) in the adsorption of cationic red 14 dye. In our experimental-laboratory study, the changes in removal efficiency were assessed by considering the changes in values of pH, concentration, adsorbent dose, contact time, and temperature. In addition, the nature of our prepared adsorbent was defined based on scanning electron microscopy (SEM), Brunauer–Emmett–Teller (BET), X-ray diffraction (XRD), and Fourier-transformed infrared (FTIR) spectroscopy techniques. The concentration of dye after the completion of experiments was recorded using a spectrophotometer at 514 nm. Evaluating the attained data by isotherm and kinetic models were also considered. Our results demonstrated the enhancement in the efficiency of the studied process at higher contact times, temperatures, and pH and its decline at higher initial dye concentrations. pH = 11, time of 45 min, dye concentration of 50 mg/L, and AC mass of 0.25 g/l were optimal values in obtaining the highest removal of the studied dye. Langmuir isotherm and pseudo-second-order (PSO) with ( $R^2 = 0.9972$ ) and ( $R^2 = 0.9947$ ) were the best isotherms and kinetic models in the description of the observed data, respectively. Considering the results, CWAC could be effectively utilized for the adsorption of cationic red 14 dye from solutions.

**Keywords** Adsorption · Activated carbon · Cationic red 14 dye · Isotherms · Kinetics

## Introduction

The water shortage, as a problem of recent decades, has been exacerbated by the discharge of untreated wastewater, especially wastewater containing organic dye (Saeed et al. 2010; Rahmani et al. 2022; Seidmohammadi et al. 2019). Available reports have been representative of producing 1.6 million tons of color compounds annually and entering 10 to 15% of this volume into the environment without any treatment process (Tan et al. 2015; Mohammadifard et al. 2022; Ghanbari et al. 2022). Color compounds from various industries including textiles, paper printing, food, and cosmetics are discharged into the environment (Shi et al. 2007; Hasani et al. 2021). Their presence in drinking water has been found to be associated with severe effects on vital human organs such as the brain, liver, kidneys, and central nervous system (Mohammed et al. 2014). These compounds are toxic, mutagenic, and carcinogenic, and on the other

---

✉ Mehdi Vosoughi  
mvn\_20@yahoo.com

✉ Abdollah Dargahi  
a.dargahi29@yahoo.com

<sup>1</sup> Students Research Committee, Ardabil University of Medical Sciences, Ardabil, Iran  
<sup>2</sup> Department of Environmental Health Engineering, School of Public Health, Ardabil University of Medical Sciences, Ardabil, Iran  
<sup>3</sup> Social Determinants of Health Research Center, Ardabil University of Medical Sciences, Ardabil, Iran  
<sup>4</sup> Department of Environmental Health, Khalkhal University of Medical Sciences, Khalkhal, Iran

hand, due to the reduction in light transmission permeability into aqueous media, reduce photosynthesis, and lack of dissolved oxygen in the lower layers (Singh et al. 2011; Wang et al. 2008; Royer et al. 2009). Even trivial dye amounts (about 1 mg/l) in drinking water can make it unsuitable for human consumption (Salleh et al. 2011). Among different dyes used in the textile industries, the cationic 14 red dye has been found to be one of the most widely used and important cationic dyes (Naghizade Asl et al. 2016). Reducing and eliminating these pollutants is a remarkable subject and should be implemented before their discharge into aquatic environments (Salman 2009; Peyghami et al. 2021). Hence, a variety of methods are used to remove cationic red 14 dye from aqueous media. These methods include ion exchange, membrane processes, electrochemical degradation, ozonation, and adsorption (Hameed and El-Khaiary 2008; Qu et al. 2008). However, these methods have limitations, such as the production of excess sludge, the time-consuming fermentation process, and the inability to remove colored compounds continuously (Robinson et al. 2001).

Among these, the adsorption process due to its compatibility with the environment is one of the most attractive and at the same time the most effective methods for removing dyes (Qadri et al. 2009). The adsorption process is considered as a high-performance process for various reasons such as no production of hazardous materials and free radicals, reusability, simplicity, and flexibility in operation (Shen et al. 2011; Zhao et al. 2010). Minerals such as clay (Lambert et al. 1997), coconut husk (Vieira et al. 2011), magnesium chloride (Gao et al. 2007), sugarcane pulp ash (Mall et al. 2005a), oxyhumilite (McKay et al. 1999; Janoš et al. 2005), rice husk ash (Mane et al. 2007), and activated carbon (AC) (Malik 2004) have been used to adsorb pigments.

AC has been found a widespread application in removing contaminants from aqueous solutions; this widespread application is related to its specific surface area and high adsorption capacity, stable chemical properties, easy availability and handling, and high efficiency (Sobhanardakani and Zandipak 2016) Despite the advantages mentioned for AC, disadvantages such as the cost of production materials have limited the use of AC on a real scale. To solve the

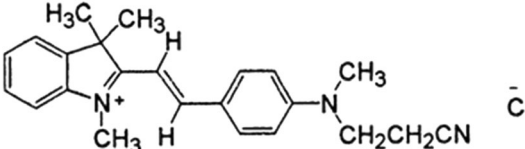
mentioned problem, low-priced materials, e.g., agricultural wastes, have been considered as a potential option (Bazrafshan and Kord 2013) and has chosen as a subject for many studies. For example, Bijari et al. prepared AC from grape shrub waste to remove reactive dye from Black 5 (Bijari et al. 2018). Moreover, Mousavi et al. have used AC prepared from the leaves of Grape trees to adsorb methylene blue bleach (Mousavi et al. 2016).

Our search among the available reports could exhibit the lack of documents on the use of AC prepared from cherry wood (CW) to adsorb the cationic red 14 dye. Therefore, preparing AC prepared from CW (CWAC) by chemical activation and its employment for eliminating cationic red 14 dye from aqueous solutions was considered as the main objective of our study. Based on this sub-objective of the present study was as follows: (a) determining functional and surface properties of the prepared AC; (c) defining optimal conditions employed for assessing the influence of pH, time, initial dye levels, AC mass, and temperature; (d) documenting adsorption equilibrium, isotherms, and adsorption kinetics for dye adsorption; (e) evaluating AC recyclability with HNO<sub>3</sub> and NaOH in 5 cycles, and (f) comparing optimal conditions with actual wastewater.

## Materials and methods

Cationic red 14 dye as a precursor of dye and other chemicals were purchased from Alvan Sabet Company in Hamedan and Merck Company in Germany, respectively. The general characteristics of cationic red 14 dye are reported in Table 1 (Vinitnantharat et al. 2008). Sodium hydroxide (NaOH) and 0.1 N sulfuric acid (H<sub>2</sub>SO<sub>4</sub>) were the solutions that were employed for adjusting the pH. Double distilled water was utilized for preparing and diluting the solutions in all steps of the study. In our study, evaluating the performance of the adsorption process was also done by considering the changes in values of factors including pH, prepared AC mass, time, and studied dye concentration. Lastly, studies related to isotherm and kinetics of the process were conducted.

**Table 1** Properties and chemical structure of the cationic red 14 dye

Molecular structure	Molecular weight (g/mol)	Wavelength (nm)	Chemical formula	Scientific name
	379.43	514	C <sub>23</sub> H <sub>26</sub> ClN <sub>3</sub>	Basic red 14 (BR14)

## Adsorbent preparation

Cherry wood (CW) was collected from gardens around Meshkinshahr, Iran. CW was chopped into small pieces. In the next step, to remove contaminants and impurities, the chopped pieces underwent a washing process several times with distilled water. It was impregnated with 85% phosphoric acid for 24 h at room temperature. It was then transported to a cylindrical metal reactor with a cylindrical lid and exposed to a temperature of 650 °C for 2 h Table 2.

After withdrawing the reactor from the furnace, the AC was rinsed with distilled water until neutralizing its pH and exposed to a drying process at 105 °C for 24 h, using an oven. Eventually, after sieving the prepared AC with a 20–30 mesh sieve, it was pulverized and stored (Mahvi and Heibati 2010).

## Determining the nature of activated carbon

Investigating the structural properties and identifying the formed phases was performed through the employment of XRD analysis. For this analysis, the Philips device made in the Netherlands in the range of  $2\theta$  between 10 and 80 degrees with a scanning speed of 0.01 s per degree was used. The surface morphology of the synthetic samples was scanned by SEM analysis using TESCA MIRA III. Preparing Fourier Infrared (FTIR) assay was done based on potassium bromide (KBr) as a reference; its analysis with a resolution of 1.1 cm was performed in various diagnoses from 450 to 450  $\text{cm}^{-1}$ . Also, nitrogen adsorption/desorption isotherms were performed using BET (II BELSORP mini) analysis at 77 °C; by this analysis, the pore volume and specific surface area of AC were defined.

## Test method

In the first stage of this study, preparing stock solution (1000 mg/l) was done via dissolving powder of cationic red 14 dye in double distilled water. Experiments of adsorption were designed based on defining different values of effective parameters, e.g., initial pH, prepared AC mass, time, initial dye concentration, and temperature. After regulating the solution pH, a known amount of AC was poured into the solution, and the solution was exposed to a stirring process at 250 rpm until the completion of the process. After that centrifuging the solution was considered to be at 3,000 rpm for 5 min. Dye absorbance at 514 nm was read using a spectrophotometer (Naghizade

Asl et al. 2016). Equations No. 1 and 2 are employed for calculating the dye removal percentage and the amount of dye adsorbed per unit mass of adsorbent ( $q_e$ , mg/g): (Rashtbari et al. 2018; Afshin et al. 2018; Shokoochi et al. 2018):

$$R = \frac{C_0 - C_t}{C_0} \times 100 \quad (1)$$

$$q_e = \frac{C_0 - C_t}{M} \times V \quad (2)$$

In mentioned equations, the dye removal percentage was shown by  $R$ .  $C_0$  (mg/l) and  $C_t$  (mg/l) were used to symbolize the dye concentration in the solution at the start and end of the process, respectively.  $q_e$  (mg/g) represented adsorbent adsorption capacity,  $V$  (L) indicated solution volume and  $M$  (g) was the mass of the adsorbent.

## Determination of $\text{pH}_{\text{zpc}}$

The  $\text{pH}_{\text{zpc}}$  test was performed to investigate the surface charge of activated carbon. To determine  $\text{pH}_{\text{zpc}}$ , three solutions, i.e., 0.01 M sodium chloride salt solution and sulfuric acid and sodium solutions, were initially prepared; the first solution was used as electrolyte and two other solutions were the agents of pH control. After adjusting the pH of dye solutions to values from 2 to 12 and addition of 0.01 g/l adsorbent to them in the 100 ml Erlenmeyer flasks, the mixing process was considered for them at 150 rpm for 48 h. The observed pH after the mentioned period was recorded as final pH and was drawn against initial pH values to define the  $\text{pH}_{\text{zpc}}$  point of the adsorbent, which was the intersection point of the lines with the straight line (Leili et al. 2018).

## Results and discussion

### Investigation of the structural nature of the AC

#### FTIR analysis

FTIR images for activated carbon before and after the cationic red 14 dye adsorption process for determining the vibrational frequency changes in the functional groups are shown in Fig. 1a.

The frequency spectrum was measured at 450–4000  $\text{cm}^{-1}$ . The FTIR spectrum disclosed the peaks at 1176, 1574, and 1648 related to the C–O bond tension of carboxylic acid, C=O and C=C, respectively, and peaks at 2937–2855 and 3446–3427 indicating the H–C and O–H bonds, respectively.

**Table 2** BET analysis results for activated carbon

Material	$S_{\text{BET}}$ ( $\text{m}^2/\text{g}$ )	$S_{\text{micro}}$ ( $\text{m}^2/\text{g}$ )	$S_{\text{meso}}$ ( $\text{m}^2/\text{g}$ )	$V_{\text{Total}}$ ( $\text{cm}^3/\text{g}$ )	$D_p$ (nm)
AC	738.17	525.53	212.64	0.558	3.0237

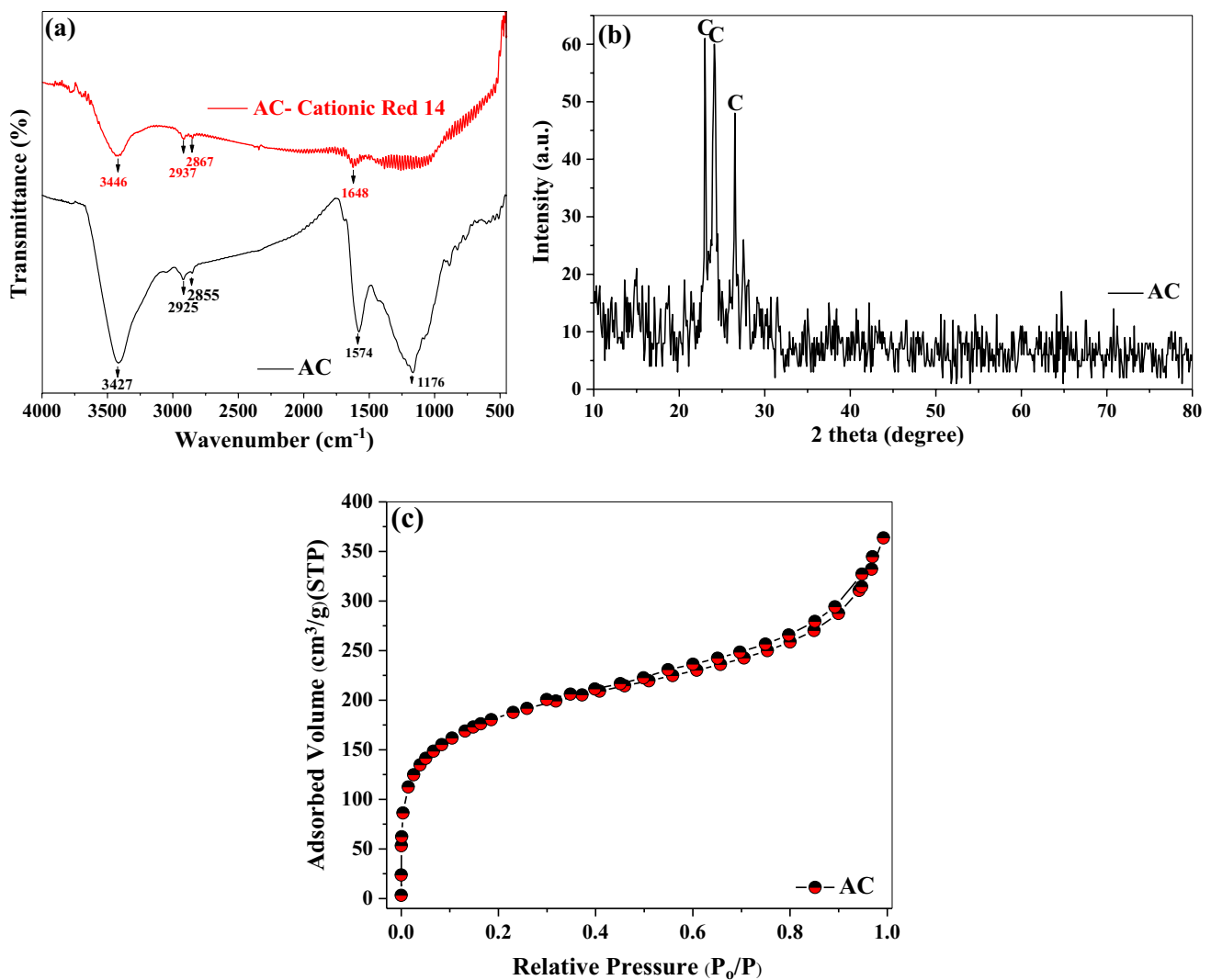


Fig. 1 RITF spectrum (a), XRD analysis (b) and nitrogen adsorption and desorption isotherm on activated carbon (c)

### XRD analysis

Findings related to this analysis for prepared AC are published in Fig. 1b. According to this analysis, the peaks in the range  $2\theta$  equal to 23.61, 24.1, and 27.5 are correspondent to the existence of carbon in the structure of CWAC.

### Brunauer–Emmett–Teller (BET)

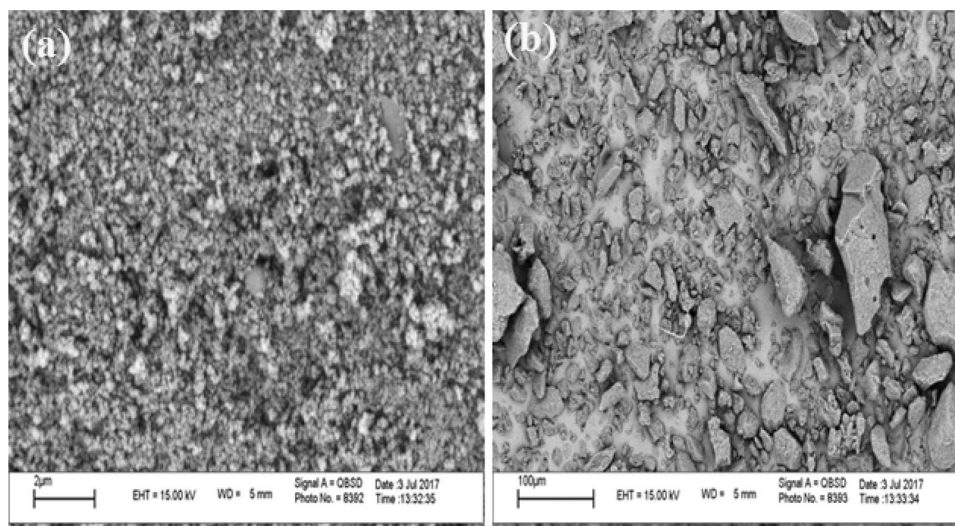
According to the analysis of this part, the pore volume and the specific surface area of our prepared AC were defined. The isotherm of nitrogen gas adsorption–desorption on our evaluated AC is provided in Fig. 1c. Comparison of obtained results with the IUPAC (International Union of

Pure and Applied Chemistry) classification revealed the consistency of adsorption–desorption isotherms with type IV of AC. Moreover, CWAC has a specific surface area of 738.17 square meters per gram, and the total pore volume is 0.558 cubic centimeters per gram. Also, the average diameter of AC pores is 0.2337 nm, which indicates the cavities of this adsorbent in the mesoporous area.

### Investigation of adsorbent morphology using SEM analysis

SEM images for studied AC before and after the process of adsorption of cationic red 14 dye are represented in Fig. 2a and b, respectively. According to our observations, there was a consistency between surface microparticles on

**Fig. 2** SEM images of activated carbon before (a) and after the surface adsorption process (b)



CWAC and other available reports represented by previous studies (Bijari et al. 2018; Nourmoradi and Noori 2015). SEM images were indicative of favorable porosity of the surface of the evaluated AC (Ghasemi 2018). As can be seen, the sharp adsorbent surfaces are coated with cationic red 14 dye to create smooth surfaces.

#### The effect of the solution pH and $pH_{zpc}$

The pH of the solution is able to alter the adsorbent surface charge, the degree of ionization of the adsorbent, and the active adsorbent groups (Dargahi et al. 2022). Hence, changes in the initial pH of the solution can exhibit a remarkable share in the dye removal process. Considering results related to  $pH_{zpc}$  and the effect of the initial pH on the efficiency of evaluated process reported in Fig. 3a, b, at different pH, an initial cationic red 14 dye level of 50 mg/l, a fixed AC mass of 0.1 g/l, a time of 30 min at 25 °C, an enhancement in the efficiency could be noticed by rising pH; so that it enhanced from 14 to 53.5% for pH increase from 3 to 11. Based on our result, the optimum pH was a pH of 11 for other experiments. In order to confirm the obtained results, it is necessary to know that the activated carbon at  $pH_{zpc}$  is equal to 6.8 of the uncharged state, and at this pH, the adsorbent surface is affected by positive and negative charges equally. It should be noted that when the pH decreases, the adsorbent surface becomes positively charged due to the absorption of  $H^+$  ions, and the dye removal efficiency decreases. But in conditions where  $pH_{zpc} < pH$ , the reverse of the process occurs, in other words, the adsorbent surface is negatively charged and the interaction between the adsorbent and the dye molecules increases. At acidic pH, high concentrations of hydrogen ions cause the adsorbent to hold a more positive charge; this thwarts the adsorption of cationic dyes on the adsorbent. In other words, there will

be a competition between extra hydrogen ions and cationic dye molecules for adsorption on active sites. Consequently, a substantial decrease is recognized in the  $q_e$  of the adsorbent at low pH values. According to the FTIR results obtained for CWAC, different functional groups such as carbonyl and hydroxyl are influenced by pH. On the other hand, carboxylic acid in the structure of AC has acidic properties and the viscosity of the skin surface of fruits is due to the presence of this factor, which increases the absorption potential of cationic red 14 dye (Pavan et al. 2008). Carbonyl functional groups (C=O) due to the negative charge in their structure allow for adsorbing cationic red 14 dye with a positive charge. Our results exhibited to have similarity to the research findings of Powell et al., who evaluated the adsorption of anionic and cationic dyes on volatile ash. In this study, it was recognized that removing cationic and anionic dyes developed and diminished with increasing pH, respectively. Loading of volatile ash adsorbent with negative charges at high pH has led to better removal of cationic dyes at high pH while loading of volatile ash adsorbent surface with positive charges at low pH values has resulted in high adsorption of anionic dyes at low pH (Janoš et al. 2003). According to (Naghizade Asl et al. 2016), by increasing the pH, the removal of basal dyes of purple 16 and cationic red 14 enhanced.

#### The effect of the adsorbent mass

The results of the dye adsorption efficiencies for different CWAC amounts of 0.025, 0.05, 0.1, 0.25, 0.35, and 0.5 g/l are displayed in Fig. 3c. Based on these findings, increasing the CWA amounts has participated in developing cationic red 14 dye removal because of rising the number of active adsorption sites available against a constant amount of dye level. Rising the adsorbent dose has been found to be



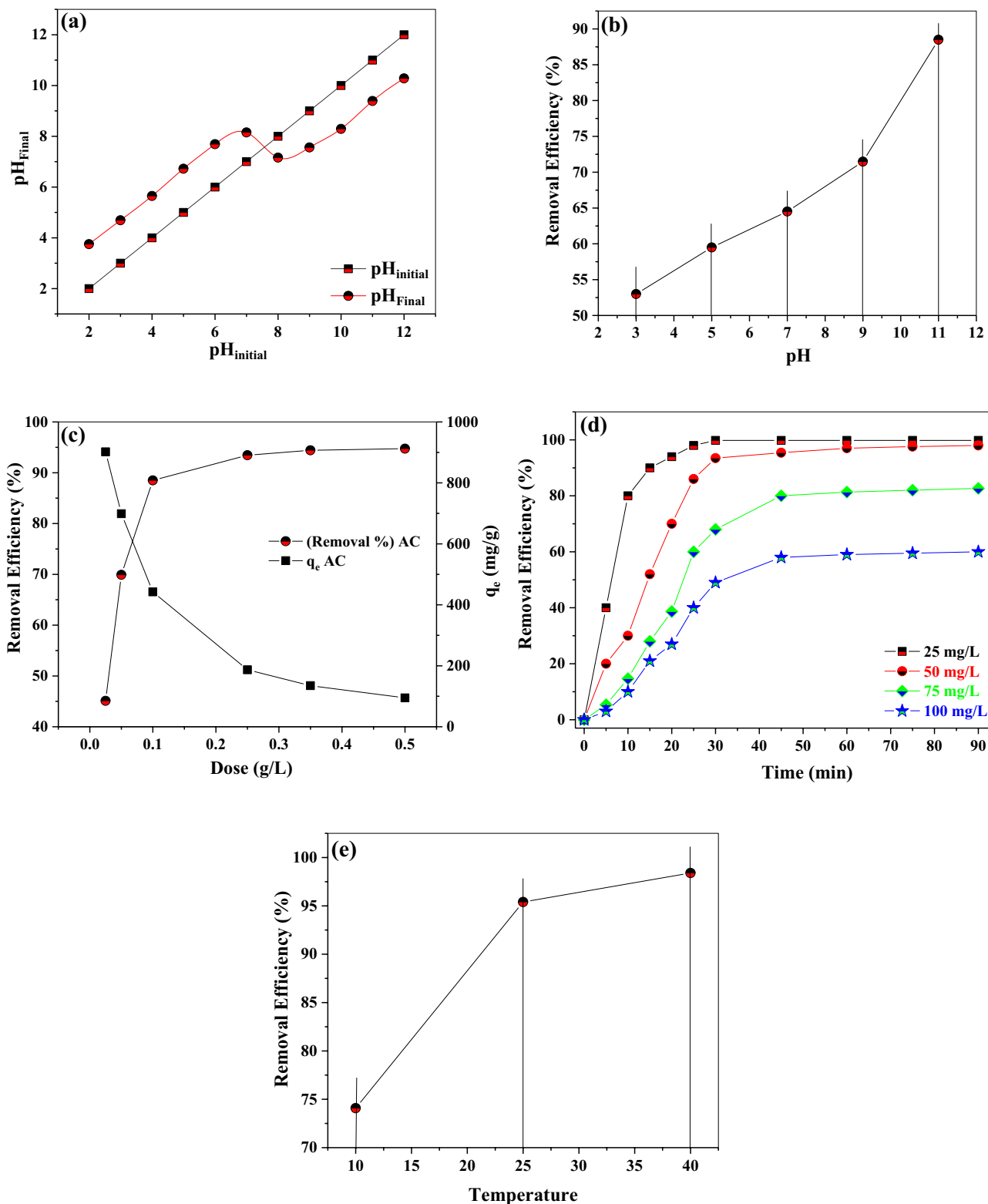


**Fig. 3**  $pH_{zpc}$  diagram of activated carbon (a), effect of pH changes (b), effect of adsorbent dose changes (c), effect of initial dye concentration (d) and effect of temperature on the absorption of cationic red 14 dye by activated carbon (e)

associated with enhancing the chance of interaction between adsorbent particles, which results in reducing its surface area and increasing the penetration path length and thus declining the adsorption density (Mall et al. 2005b). Although the amount of dye removal increases with rising adsorbent mass, a reduction in the amount of dye absorbed per gram of adsorbent ( $q_e$ ) was visible; so that when the CWAC mass increased from 0.025 to 0.5 g/l, the efficiency for 50 mg/l of dye after 30 min augmented from 45.10 to 98.74%. Also, the  $q_e$  decreased from 902 to 92 mg because the concentration of the dye solution declined due to adsorption by unsaturated active sites on the adsorbent surface and the accumulation of particles and adhesion between them caused by increasing the amount of adsorbent (Calvete et al. 2009; Shokoohi et al. 2020). Rising the AC mass to a certain amount does not lead to noteworthy development in the amount of dye removal. It seems that at a certain adsorbent mass, the highest possible absorption rate is achieved and then the amount of contaminant remaining will remain constant even with increasing dose of adsorbent (Chakravarty et al. 2010). In the study of Sentil Kumar et al., it is also reported that increasing AC mass participated in developing dye removal efficiency and diminishing  $q_e$  (Senthilkumar et al. 2006).

### The effect of the initial dye concentration

The influence of changes in the initial concentration of cationic red 14 dye on performance was explored at 25, 50, 75, and 100 mg/L (Fig. 3d). Regarding the obtained results, the percentage of cationic red dye removal dropped suggestively with increasing the initial concentration.

At a constant pH of 11, a CWAC mass of 0.25 g/l, and a temperature of 25 °C, the dye removal efficiency reduced from 100 to 59.88% for rising the pollutant concentrations from 25 to 100 mg/l. The mentioned observation is described by the fact that with increasing initial dye concentration, active sites and adsorbent capacity are limited and saturated rapidly at high concentrations of cationic red 14 dye (Karthikeyan et al. 2005). However, the amount of pollutant absorbed per unit mass of the adsorbent in the same conditions represented the opposite trend. An improvement in the  $q_e$  of the AC can also be interpreted as follows: an increase in the concentration is associated with developing the driving force of mass transfer and the rate of passage of dye molecules from the solution to the liquid layer surrounding the adsorbent and finally to the surface of the adsorbent particles (Caturla et al. 1988). In other words, enhancing the  $q_e$  is ascribed to increasing the collision between the dye-adsorbent molecules and also increasing the concentration gradient and thus accelerating the mass transfer. Mentioned evens is led to enhancing the adsorption of dye molecules by adsorbent particles and eventually developing the  $q_e$  (Hameed 2009; Al-Ghouti et al. 2009).

Shokoohi et al. also concluded a decline in removal efficiencies for higher dye concentrations, due to the fixed number of sites on a certain amount of adsorbent (Al-Ghouti et al. 2009).

In another study by Wang et al., it was recognized that the adsorption of base dyes on MCM-22 zeolite lessened for higher initial dye concentrations (Wang et al. 2006).

It is also observed that in the first minutes, the adsorption rate is high and with the passage of time, the constant removal efficiency is observed. At 45 min, the equilibrium is reached. The dye removal efficiency progressed over time for different concentrations of the studied dye. These observations were representative of the lack of notable effect for the initial levels of dye on the time needed for reaching equilibrium. The rate of rapid and high adsorption in the early times was related to existing empty active sites on the adsorbent surface, which over time, their gradual occupation by dye molecules leads to obtaining the fixed dye adsorption values. On the other hand, increasing time will be associated with difficulty in the occupation of the remaining empty areas due to the increase in repulsive forces between the dye molecules (Luo et al. 2010; Mohamed and Ouki 2011).

Amin et al. inspected the removal of reactive orange dye by three different types of ACs and stated that the adsorption of this dye on AC was done very quickly in the first minutes and over time, the removal percentage increased and the maximum removal rate took about 1 h (Amin 2008).

### The effect of the temperature

To investigate the changes in the efficiency of the evaluated process at different temperatures, experiments were performed at three temperatures of 10, 25, and 40 °C under optimal conditions (pH of 11, CWAC mass of 0.25 g, and 50 mg/l dye).

Our observations was representative of the fact that rising the temperature increases the dye removal efficiency by AC, so that by rising the temperature from 10 to 40 °C, the adsorption rate has improved from 74.08 to 98.4%. Increasing the adsorption rate with rising temperature specifies the heat absorption and the nature of the chemical adsorption process; this can be ascribed to the rise in the size of the adsorbent cavities and the enhancement in operative collisions between AC and adsorbate molecules (Namasivayam and Yamuna 1995).

## Isotherm studies and adsorption kinetics

### Adsorption kinetics

Defining the transmission quality of adsorbed molecules per unit time and studying variables that affect the reaction rate are done based on kinetic equations (pseudo-first-order

(PFO) and pseudo-second-order (PSO) models in present study); linear kinetic equations of each model are presented as Eq. 3 and 4, respectively (Dargahi et al. 2021).

$$\ln(q_e - q_t) \ln q_e - k_1 t \tag{3}$$

$$\frac{t}{q_t} = \frac{1}{K_2 q_e^2} + \frac{1}{q_e} t \tag{4}$$

In the cited equations,  $K_1$  represents the rate coefficient (1/min) and  $K_2$  indicates the PSO reaction constant (mg/gr.min).  $q_e$  and  $q_t$  show the adsorption capacity at equilibrium time and  $t$  time in mg/g, respectively.  $q_e$  and  $K_1$  are the intercept and the slope of the line graph obtained by drawing  $\ln(q_e - q_t)$  versus  $t$ , respectively. In Eq. (4), determining  $q_e$  and  $K_2$  values is based on the slope and intercept of the linear of graph  $t/q_t$  versus  $t$  (Kakavandi et al. 2013; Borna et al. 2016).

Figure 4 represents the PFO and PSO models. The parameters of PFO and PSO are presented in Table 3. According to tables, the fit of PSO (regression coefficient 0.9947) with the experimental data is superior to that of PFO.

On the other hand, the  $q_e$  predicted by the PSO has less difference relative to the experimental  $q_e$  compared to the PFO. As depicted by Table 3, the PSO constant ( $K_2$ ) decreases with increasing dye levels. The presence of sufficient sites in a constant amount of adsorbent to absorb lower concentrations of dye could lead to observing the higher adsorption rate initially. Gradually, however, the rate of adsorption of dissolved materials also decreased since for high concentrations, a reduction in required active sites happened. It was correspondent to Amin et al., who scrutinized blue-106 removal using activated carbon (Borna et al. 2016).

**Adsorption isotherms**

These models have been known as adsorption properties and equilibrium data; describing the quality of reactions that occurred between contaminants react and adsorbents is done by these models, and they effectively participate in optimizing the use of adsorbent.

The isotherm models used in the present study were Langmuir and Freundlich, which were employed for investigating the dye adsorption behavior on AC. The hypotheses represented by the Langmuir model are surface uniformity

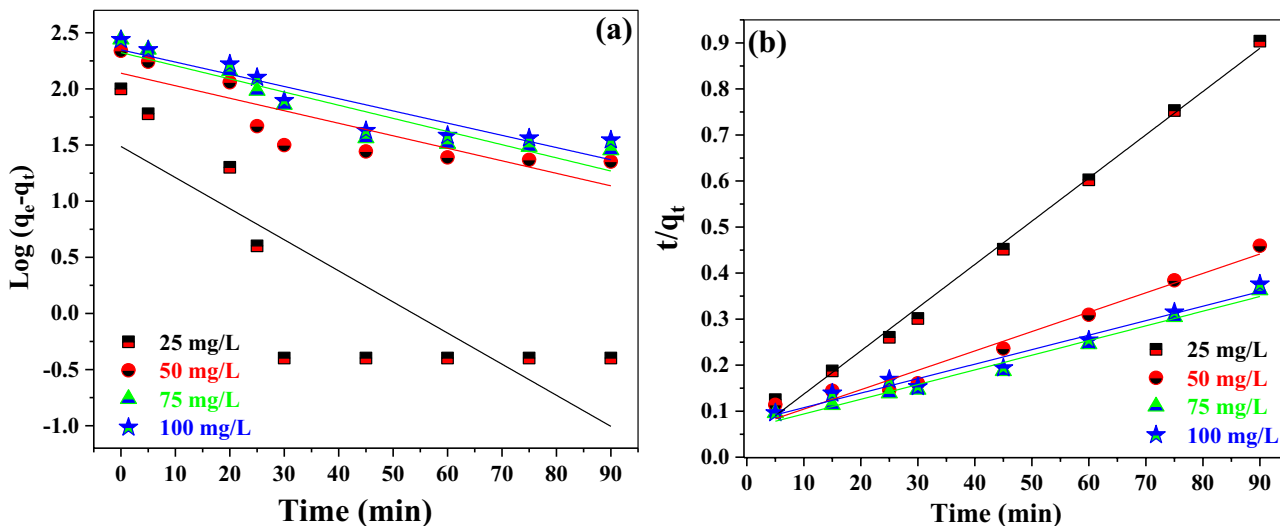


Fig. 4 Chart of quasi-first degree (a) and quasi-second degree (b) kinetic model for red cation adsorption 14

Table 3 Calculated variables for the kinetic model

Dye concentration (mg/l)	$q_{e,exp}$ (mg/g)	Quite a degree			Quasi-second degree		
		$q_{1,cal}$ (mg/g)	$k_1$ (1/min)	$R^2_1$	$q_{2,cal}$ (mg/g)	$K_2$ (g/ mg min)	$R^2_2$
25	100	293.19	0.0633	0.7045	104.17	0.0030	0.9947
50	218.5	135.15	0.0255	0.7644	222.22	0.0004	0.9644
75	276.5	135.58	0.0267	0.8847	285.71	0.00028	0.9624
100	247.5	217.82	0.0249	0.8798	285.71	0.00023	0.944



monolayer adsorption and elimination of the interaction effects of adsorbate molecules.

The Equation related to Langmuir Model, the single-layer adsorption process, is given in Eq. (5). The Freundlich model of the adsorption process is defined by Eq. (6). The Langmuir relationship was consistent with experimental experiments when the adsorption sites were uniform. If the surface is heterogeneous, the Freundlich relation obtained by quantifying the amount of material adsorption at different pressures provides a better description of the data. In this model,  $n < 1$  is indicative of poor absorption while values of 1–2 and 2–10 are representative of moderate and desirable absorption, respectively (Hao et al. 2010). Determining the values of  $n$  and  $K_f$  is accomplished based on the slope and intercept of the linear graph of  $\log q_e$  versus  $\log C_e$ , respectively.

$$\frac{C_{e_q}}{q_{e_q}} = \frac{1}{Qb} + \frac{C_{e_q}}{Q} (\%) \tag{5}$$

$$\log (q_e) = \log (K_f) + \frac{1}{n} \log (C_e) \tag{6}$$

In the represented equations above,  $q_{e_q}$  (mg/g) is the amount of dye adsorbed per gram of adsorbent and  $C_{e_q}$  (mg/l) is the equilibrium concentration of the dye in equilibrium.  $Q$  and  $b$  are Langmuir parameters;  $Q$  is related to maximum adsorption capacity and  $b$  corresponds to adsorption correlation energy (Biglari et al. 2018).  $C_e$  is used to

show equilibrium concentration (mg/L), and  $q_e$  represents adsorption capacity at equilibrium time (mg/g).  $K_f$  and  $n$  Freundlich are adsorption constants; these correspond to adsorption capacity and intensity (Niri et al. 2015). One of the properties of the Langmuir equation is the dimensionless parameter of the separation coefficient  $R_1$ ; this is employed for defining the type of adsorption process. If  $R_1 > 1$  type of adsorption is undesirable,  $R_1 = 1$  type of linear adsorption,  $1 > R_1 > 0$  optimal adsorption, and  $R_1 = 0$  adsorption is irreversible (Mahvi and Heibati 2010). The equation of separation coefficient  $R_1$  is presented in Eq. (7).

$$R_1 = \frac{1}{1 + bc} \tag{7}$$

For both studied isotherm models, plotting them was done based on the obtained data from experiments conducted under optimal conditions and results observed for the parameters represented by linear regression. Our observations were indicative of the greater consistency of data achieved by experiments with the Langmuir model diagram Fig. 5.

The correlation coefficients detected for these two models approved the higher correlation coefficient of the Langmuir model (0.9972) compared to Freundlich (0.9839); based this, the Langmuir model is introduced as a better model for unfolding the dye adsorption behavior. Therefore, the mentioned results indicate the uniform active site distribution on the adsorbent surface and subsequently the adsorbing pigment in homogeneous locations. The Langmuir and Freundlich parameters of cationic red 14 dye adsorption are

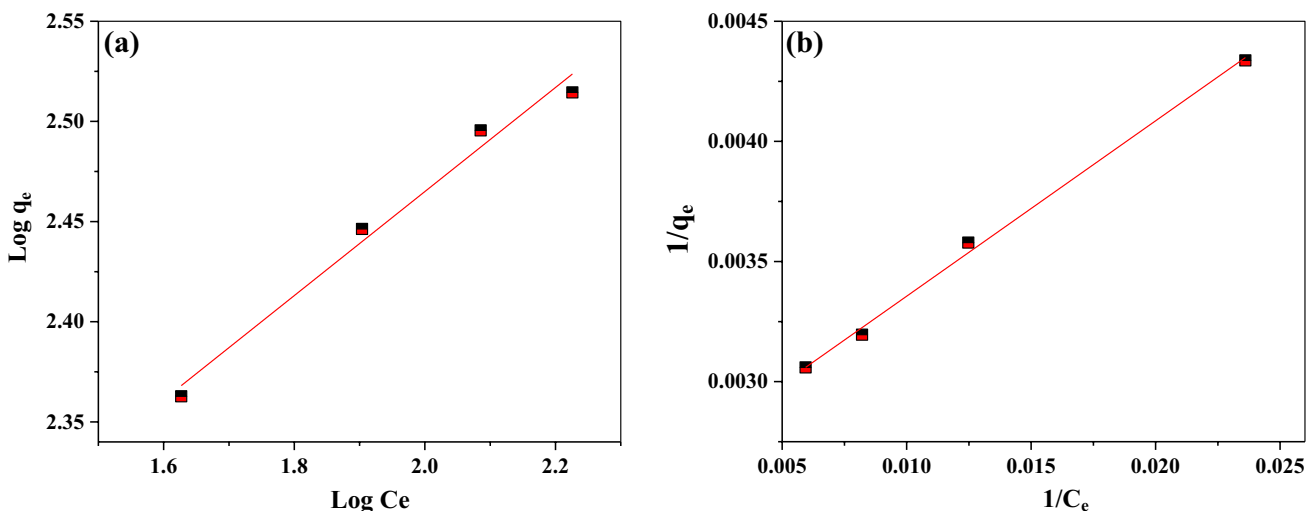


Fig. 5 Freundlich (a) and Langmuir (b) isotherm diagrams for activated carbon on red cationic dye removal efficiency 14

Table 4 Langmuir and Freundlich absorption isotherm coefficients

Model	Langmuir isotherm				Freundlich isotherm		
Parameters	$K_1$ (mg/L)	$q_m$ (mg/g)	$R^2$	$R_L$	$K_f$ (mg/L)	$n$	$R^2$
Amounts	0.0356	348.62	0.9972	0.219	88.21	3.85	0.9839

**Table 5** Comparison of  $q_e$  of different ACs for dye adsorption

Pollutant	Adsorbent	pH	$q_{\max}(\text{mg/g})$	References
Reactive black color 5	Activated carbon	2	571	McKay et al. (1999)
Red acid dye 18	Activated carbon made from walnut wood	5	30.3	Malik (2004)
Red acid color 18	Oxidized multi-walled carbon nanotubes	3	167	Namasivayam and Yamuna (1995)
Cationic red color 14	Coconut shell charcoal	11	22.93	Dargahi et al. (2021)
Blue-86 (86-BD)	Activated carbon prepared from orange peel	2	29.43	Kakavandi et al. (2013)
Cationic red color 14	Activated carbon prepared from cherry tree	11	348.61	Current study

publicized in Table 4. The maximum  $q_e$  for produced AC using the Langmuir model is 348.61 mg/g. Our findings were observed to be in-line with the reports provided by Xiao, Sential Coma, and Ahmed et al. (Senthilkumar et al. 2006; Xiao et al. 2012; Ahmad and Rahman 2011).

Table 5 compares the  $q_e$  of CWAC with studies conducted for dye removal by other adsorbents. The CWAC shows a higher  $q_e$  than AC prepared in previous studies.

### Adsorbent recovery

Having the characteristic of recoverability and reusability has been identified to be vital for adsorbents from economical and practical aspects. The employment of chemical methods for the recovery of adsorbents has recently found remarkable popularity. The findings related to the recovery and reuse of evaluated AC are depicted in Fig. 6. In chemical recovery, red cationic dye molecules 14 are dissolved in solution or replaced by ion exchange with the AC surface. NaOH ions compete with cationic red 14 dye located in active sites, and cationic red 14 dye is isolated from active sites and adsorbed. Our results confirmed the substantial potential of studied AC in the treatment of wastewater and its cost-effectiveness since it exhibited a reusability in five consecutive cycles.

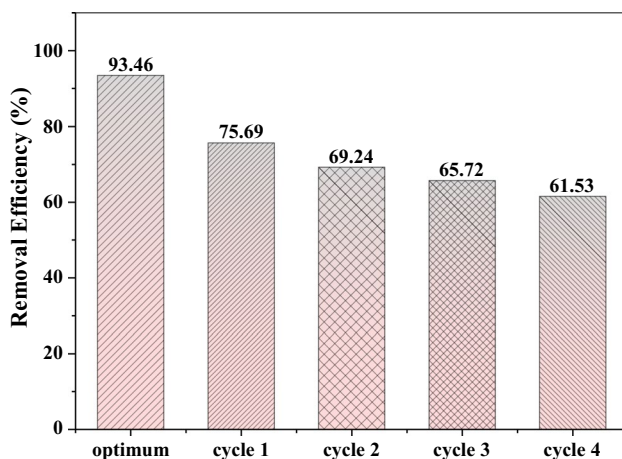


**Fig. 6** Recovery and reuse diagram for activated carbon on cationic red 14 dye removal efficiency

### Conclusion

The present study evaluates the cationic red 14 dye adsorption using CWAC. Our results were indicative of the high efficiency of our prepared AC so that it could afford significant dye removal efficiency in a short time. Enhancing dye removal efficiency by rising pH, prepared AC dose, and time was another observation in our study. Further, increasing the concentration of cationic red 14 dye has resulted in a decline in the efficiency of the process. Langmuir was found the best isotherm model, and PSO was the best kinetic model based on our observations. Generally, our findings ratified that the adsorption process using CWAC could be an operative technique for eliminating cationic red 14 dye from aqueous media.

**Acknowledgements** We hereby thank the esteemed Vice Chancellor for Student Research of Ardabil University of Medical Sciences and Ardabil Health Services for financial support of this research (design code IR.ARUMS.REC.1397.222) and esteemed colleagues in the Faculty of Health.

**Author contribution** All authors had equal contributions in writing, review, and final approval of the paper.

**Funding** The current study was financially supported by Ardabil University of Medical Sciences.

**Data availability** The dataset and analyzed during the current study are available from the corresponding authors on realistic demand.

### Declarations

**Conflict of interest** The authors declare that there is no conflict of interest regarding the publication of this work.

**Ethics approval** Not applicable.

**Consent to participate** Not applicable.

**Consent for publication** Not applicable.

**Open Access** This article is licensed under a Creative Commons Attribution 4.0 International License, which permits use, sharing, adaptation, distribution and reproduction in any medium or format, as long as you give appropriate credit to the original author(s) and the source, provide a link to the Creative Commons licence, and indicate if changes were made. The images or other third party material in this article are

included in the article's Creative Commons licence, unless indicated otherwise in a credit line to the material. If material is not included in the article's Creative Commons licence and your intended use is not permitted by statutory regulation or exceeds the permitted use, you will need to obtain permission directly from the copyright holder. To view a copy of this licence, visit <http://creativecommons.org/licenses/by/4.0/>.

## References

- Afshin S, Mokhtari SA, Vosoughi M, Sadeghi H, Rashtbari Y (2018) Data of adsorption of basic blue 41 dye from aqueous solutions by activated carbon prepared from filamentous algae. *Data Br* 21:1008–1013
- Ahmad MA, Rahman NK (2011) Equilibrium, kinetics and thermodynamic of Remazol brilliant orange 3R dye adsorption on coffee husk-based activated carbon. *Chem Eng J* 170(1):154–161
- Al-Ghouti MA, Khraisheh MA, Ahmad MN, Allen S (2009) Adsorption behaviour of methylene blue onto Jordanian diatomite: a kinetic study. *J Hazard Mater* 165(1–3):589–598
- Amin NK (2008) Removal of reactive dye from aqueous solutions by adsorption onto activated carbons prepared from sugarcane bagasse pith. *Desalination* 223(1–3):152–161
- Bazrafshan E, Kord MF (2013) Evaluation of color removal of Methylene blue from aqueous solutions using plant stem ash of Persica. *J North Khorasan Univ Med Sci* 4(4):523–532
- Biglari H, RodríguezCouto S, Khaniabadi YO, Nourmoradi H, Khoshgoftar M, Amrane A et al (2018) Cationic surfactant-modified clay as an adsorbent for the removal of synthetic dyes from aqueous solutions. *Int J Chem Reactor Eng*. <https://doi.org/10.1515/ijcre-2017-0064>
- Bijari M, Younesi H, Bahramifar N (2018) Optimization of activated carbon production by using K<sub>2</sub>CO<sub>3</sub> at different temperatures for the removal of reactive black 5 dye from aqueous solutions. *Iran J Health Environ* 10(4):483–500
- Borna MO, Pirsahab M, Niri MV, Mashizie RK, Kakavandi B, Zare MR et al (2016) Batch and column studies for the adsorption of chromium (VI) on low-cost hibiscus *Cannabinus kenaf*, a green adsorbent. *J Taiwan Inst Chem Eng* 68:80–89
- Calvete T, Lima EC, Cardoso NF, Dias SL, Pavan FA (2009) Application of carbon adsorbents prepared from the Brazilian pineapple-shell for the removal of Procion Red MX 3B from aqueous solution—Kinetic, equilibrium, and thermodynamic studies. *Chem Eng J* 155(3):627–636
- Caturla F, Martín-Martínez J, Molina-Sabio M, Rodríguez-Reinoso F, Torregrosa R (1988) Adsorption of substituted phenols on activated carbon. *J Colloid Interface Sci* 124(2):528–534
- Chakravarty P, Sarma NS, Sarma H (2010) Removal of lead (II) from aqueous solution using heartwood of *Areca catechu* powder. *Desalination* 256(1–3):16–21
- Dargahi A, Barzoki HR, Vosoughi M, Mokhtari SA (2022) Enhanced electrocatalytic degradation of 2, 4-dinitrophenol (2, 4-DNP) in three-dimensional sono-electrochemical (3D/SEC) process equipped with Fe/SBA-15 nanocomposite particle electrodes: degradation pathway and application for real wastewater. *Arab J Chem* 15(5):103801
- Dargahi A, Samarghandi MR, Shabanloo A, Mahmoudi MM, Nasab HZ (2021) Statistical modeling of phenolic compounds adsorption onto low-cost adsorbent prepared from aloe vera leaves wastes using CCD-RSM optimization: effect of parameters, isotherm, and kinetic studies. *Biomass Convers Biorefinery* 1–15
- Gao B-Y, Yue Q-Y, Wang Y, Zhou W-Z (2007) Color removal from dye-containing wastewater by magnesium chloride. *J Environ Manage* 82(2):167–172
- Ghanbari M, Dargahi A, Ahmadi M, Ghafari S, Jaafarzadeh N, Jorfi S (2022) Biodegradation of acid orange 7 dye using consortium of novel bacterial strains isolated from Persian Gulf water and soil contaminated with petroleum compounds. *Biomass Convers Biorefinery*
- Ghasemi S (2018) Cationic dye adsorption from aqueous soluble using activated carbon of Grapefruit peel, optimized by Taguchi method. *Modares Civ Eng J* 18(1):55–67
- Hameed B (2009) Evaluation of papaya seeds as a novel non-conventional low-cost adsorbent for removal of methylene blue. *J Hazard Mater* 162(2–3):939–944
- Hameed B, El-Khaiary M (2008) Equilibrium, kinetics and mechanism of malachite green adsorption on activated carbon prepared from bamboo by K<sub>2</sub>CO<sub>3</sub> activation and subsequent gasification with CO<sub>2</sub>. *J Hazard Mater* 157(2–3):344–351
- Hao Y-M, Man C, Hu Z-B (2010) Effective removal of Cu (II) ions from aqueous solution by amino-functionalized magnetic nanoparticles. *J Hazard Mater* 184(1–3):392–399
- Hasani K, Moradi M, Mokhtari SA, Dargahi A, Vosoughi M (2021) Degradation of basic violet 16 dye by electro-activated persulfate process from aqueous solutions and toxicity assessment using microorganisms: determination of by-products, reaction kinetic and optimization using Box-Behnken design. *Int J Chem Reactor Eng* 19(3):261–275
- Janoš P, Buchtova H, Rýznarová M (2003) Sorption of dyes from aqueous solutions onto fly ash. *Water Res* 37(20):4938–4944
- Janoš P, Sedivý P, Rýznarová M, Grötschelová S (2005) Sorption of basic and acid dyes from aqueous solutions onto oxihumolite. *Chemosphere* 59(6):881–886
- Kakavandi B, Rezaei Kalantary R, Esrafilí A, Jonidi Jafari A, Azari A (2013) Isotherm, kinetic and thermodynamic of reactive blue 5 (RB5) dye adsorption using Fe<sub>3</sub>O<sub>4</sub> nanoparticles and activated carbon magnetic composite. *J Color Sci Technol* 7(3):237–248
- Karthikeyan T, Rajgopal S, Miranda LR (2005) Chromium (VI) adsorption from aqueous solution by Hevea Brasilinesis sawdust activated carbon. *J Hazard Mater* 124(1–3):192–199
- Lambert S, Graham N, Sollars C, Fowler G (1997) Evaluation of inorganic adsorbents for the removal of problematic textile dyes and pesticides. *Water Sci Technol* 36(2–3):173–180
- Leili M, Fazlzadeh M, Bhatnagar A (2018) Green synthesis of nano-zero-valent iron from Nettle and Thyme leaf extracts and their application for the removal of cephalexin antibiotic from aqueous solutions. *Environ Technol* 39(9):1158–1172
- Luo P, Zhao Y, Zhang B, Liu J, Yang Y, Liu J (2010) Study on the adsorption of neutral red from aqueous solution onto halloysite nanotubes. *Water Res* 44(5):1489–1497
- Mahvi A H, Heibati B (2010) Removal efficiency of azo dyes from textile effluent using activated carbon made from walnut wood and determination of isotherms of acid red 18. *J Health* 1(3):7–15
- Malik P (2004) Dye removal from wastewater using activated carbon developed from sawdust: adsorption equilibrium and kinetics. *J Hazard Mater* 113(1–3):81–88
- Mall ID, Srivastava VC, Agarwal NK, Mishra IM (2005a) Adsorptive removal of malachite green dye from aqueous solution by bagasse fly ash and activated carbon-kinetic study and equilibrium isotherm analyses. *Colloids Surf A* 264(1–3):17–28
- Mall ID, Srivastava VC, Agarwal NK, Mishra IM (2005b) Removal of congo red from aqueous solution by bagasse fly ash and activated carbon: kinetic study and equilibrium isotherm analyses. *Chemosphere* 61(4):492–501
- Mane VS, Mall ID, Srivastava VC (2007) Kinetic and equilibrium isotherm studies for the adsorptive removal of brilliant green dye from aqueous solution by rice husk ash. *J Environ Manage* 84(4):390–400

- McKay G, Porter J, Prasad G (1999) The removal of dye colours from aqueous solutions by adsorption on low-cost materials. *Water Air Soil Pollut* 114(3):423–438
- Mohamed M, Ouki SK (2011) Kinetic and removal mechanisms of ethylbenzene from contaminated solutions by chitin and chitosan. *Water Air Soil Pollut* 220(1):131–140
- Mohammadifard A, Allouss D, Vosoughi M, Dargahi A, Moharrami A (2022) Synthesis of magnetic Fe<sub>3</sub>O<sub>4</sub>/activated carbon prepared from banana peel (BPAC@ Fe<sub>3</sub>O<sub>4</sub>) and salvia seed (SSAC@ Fe<sub>3</sub>O<sub>4</sub>) and applications in the adsorption of basic blue 41 textile dye from aqueous solutions. *Appl Water Sci* 12(5):88
- Mohammed M, Shitu A, Ibrahim A (2014) Removal of methylene blue using low cost adsorbent: a review. *Res J Chem Sci ISSN* 2231:606X
- Mousavi S, Khashij M, Shahbazi P (2016) Adsorption isotherm study and factor affected on methylene blue decolorization using activated carbon powder prepared grapevine leaf. *J Saf Promot Inj Prev*
- Naghizade Asl M, Mahmodi NM, Teymouri P, Shahmoradi B, Rezaee R, Maleki A (2016) Adsorption of organic dyes using copper oxide nanoparticles: isotherm and kinetic studies. *Desalin Water Treat* 57(52):25278–25287
- Namasivayam C, Yamuna R (1995) Adsorption of chromium (VI) by a low-cost adsorbent: biogas residual slurry. *Chemosphere* 30(3):561–578
- Niri MV, Mahvi AH, Alimohammadi M, Shirmardi M, Golastanifar H, Mohammadi MJ et al (2015) Removal of natural organic matter (NOM) from an aqueous solution by NaCl and surfactant-modified clinoptilolite. *J Water Health* 13(2):394–405
- Nourmoradi HA, Noori MZ (2015) Investigation on the efficacy of activated carbon modified with zinc oxide nanoparticles to remove methylene blue dye from synthetic wastewater: kinetic and isotherm study. *J Health Sys Res* 11(2):382–397
- Pavan FA, Mazzocato AC, Gushikem Y (2008) Removal of methylene blue dye from aqueous solutions by adsorption using yellow passion fruit peel as adsorbent. *Biores Technol* 99(8):3162–3165
- Peyghami A, Moharrami A, Rashtbari Y, Afshin S, Vosoughi M, Dargahi A (2021) Evaluation of the efficiency of magnetized clinoptilolite zeolite with Fe<sub>3</sub>O<sub>4</sub> nanoparticles on the removal of basic violet 16 (BV16) dye from aqueous solutions. *J Dispers Sci Technol*. <https://doi.org/10.1080/01932691.2021.1947847>
- Qadri S, Ganoe A, Haik Y (2009) Removal and recovery of acridine orange from solutions by use of magnetic nanoparticles. *J Hazard Mater* 169(1–3):318–323
- Qu S, Huang F, Yu S, Chen G, Kong J (2008) Magnetic removal of dyes from aqueous solution using multi-walled carbon nanotubes filled with Fe<sub>2</sub>O<sub>3</sub> particles. *J Hazard Mater* 160(2–3):643–647
- Rahmani AR, Gilan RA, Asgari G, Leili M, Dargahi A (2022) Enhanced degradation of Rhodamine B dye by fenton/peracetic acid and photo-fenton/peracetic acid processes. *Int J Chem Reactor Eng* 20(12):1251–1260
- Rashtbari Y, Hazrati S, Afshin S, Fazlzadeh M, Vosoughi M (2018) Data on cephalixin removal using powdered activated carbon (PPAC) derived from pomegranate peel. *Data Brief* 20:1434–1439
- Robinson T, McMullan G, Marchant R, Nigam P (2001) Remediation of dyes in textile effluent: a critical review on current treatment technologies with a proposed alternative. *Biores Technol* 77(3):247–255
- Royer B, Cardoso NF, Lima EC, Vaghetti JC, Simon NM, Calvete T et al (2009) Applications of Brazilian pine-fruit shell in natural and carbonized forms as adsorbents to removal of methylene blue from aqueous solutions—Kinetic and equilibrium study. *J Hazard Mater* 164(2–3):1213–1222
- Saeed A, Sharif M, Iqbal M (2010) Application potential of grapefruit peel as dye sorbent: kinetics, equilibrium and mechanism of crystal violet adsorption. *J Hazard Mater* 179(1–3):564–572
- Salleh MAM, Mahmoud DK, Karim WAWA, Idris A (2011) Cationic and anionic dye adsorption by agricultural solid wastes: a comprehensive review. *Desalination* 280(1–3):1–13
- Salman MS (2009) Removal of sulfate from waste water by activated carbon. *Al-Khwarizmi Eng J* 5(3):72–76
- Seidmohammadi A, Asgari G, Dargahi A, Leili M, Vaziri Y, Hayati B et al (2019) A comparative study for the removal of methylene blue dye from aqueous solution by novel activated carbon based adsorbents. *Prog Color Colorants Coat* 12(3):133–144
- Senthilkumaar S, Kalaamani P, Porkodi K, Varadarajan P, Subburaam C (2006) Adsorption of dissolved reactive red dye from aqueous phase onto activated carbon prepared from agricultural waste. *Biores Technol* 97(14):1618–1625
- Shen S, Ren J, Chen J, Lu X, Deng C, Jiang X (2011) Development of magnetic multiwalled carbon nanotubes combined with near-infrared radiation-assisted desorption for the determination of tissue distribution of doxorubicin liposome injects in rats. *J Chromatogr A* 1218(29):4619–4626
- Shi B, Li G, Wang D, Feng C, Tang H (2007) Removal of direct dyes by coagulation: the performance of preformed polymeric aluminum species. *J Hazard Mater* 143(1–2):567–574
- Shokoohi R, Gillani RA, Mahmoudi MM, Dargahi A (2018) Investigation of the efficiency of heterogeneous Fenton-like process using modified magnetic nanoparticles with sodium alginate in removing Bisphenol A from aquatic environments: kinetic studies. *Desalination Water Treat* 101:185–192
- Shokoohi R, Dargahi A, Gilan RA, Nasab HZ, Zeynalzadeh D, Mahmoudi MM (2020) Magnetic multi-walled carbon nanotube as effective adsorbent for ciprofloxacin (CIP) removal from aqueous solutions: isotherm and kinetics studies. *Int J Chem Reactor Eng*. <https://doi.org/10.1515/ijcre-2019-0130>
- Singh KP, Gupta S, Singh AK, Sinha S (2011) Optimizing adsorption of crystal violet dye from water by magnetic nanocomposite using response surface modeling approach. *J Hazard Mater* 186(2–3):1462–1473
- Sobhanardakani S, Zandipak R (2016) Removal of methyl orange dye from aqueous solutions using NiFe<sub>2</sub>O<sub>4</sub> nanoparticles: equilibrium and kinetic studies. *Iranian J Health Environ* 9(2):247–258
- Tan KB, Vakili M, Horri BA, Poh PE, Abdullah AZ, Salamatinia B (2015) Adsorption of dyes by nanomaterials: recent developments and adsorption mechanisms. *Sep Purif Technol* 150:229–242
- Vieira AP, Santana SA, Bezerra CW, Silva HA, Chaves JA, Melo JC et al (2011) Removal of textile dyes from aqueous solution by babassu coconut epicarp (*Orbignya speciosa*). *Chem Eng J* 173(2):334–340
- Vinitnantharat S, Chartthe W, Pinisakul A (2008) Toxicity of reactive red 141 and basic red 14 to algae and waterfleas. *Water Sci Technol* 58(6):1193–1198
- Wang S, Li H, Xu L (2006) Application of zeolite MCM-22 for basic dye removal from wastewater. *J Colloid Interface Sci* 295(1):71–78
- Wang K-s, Chen H-Y, Huang L-C, Su Y-C, Chang S-H (2008) Degradation of Reactive Black 5 using combined electrochemical degradation-solar-light/immobilized TiO<sub>2</sub> film process and toxicity evaluation. *Chemosphere* 72(2):299–305
- Xiao H, Peng H, Deng S, Yang X, Zhang Y, Li Y (2012) Preparation of activated carbon from edible fungi residue by microwave assisted K<sub>2</sub>CO<sub>3</sub> activation—Application in reactive black 5 adsorption from aqueous solution. *Biores Technol* 111:127–133
- Zhao C, Deng H, Li Y, Liu Z (2010) Photodegradation of oxytetracycline in aqueous by 5A and 13X loaded with TiO<sub>2</sub> under UV irradiation. *J Hazard Mater* 176(1–3):884–892

**Publisher's Note** Springer Nature remains neutral with regard to jurisdictional claims in published maps and institutional affiliations.